

Advanced ultrasonic blade root examination Analytical process and Modelling to handle examination on complex geometry

Pilani NDVOLHU¹, Dion AGOSTINHO¹, Jean Michel PUYBOUFFAT¹,
Nicolas GACHADOIT²

¹ NDT department Rotek Engineering, Johannesburg, South Africa e-mail: Dion.Agostinho@eskom.co.za

² MapleSoft France Support technique 35, Rue des Chantiers - 78000 Versailles France e-mail :
ngachadoit@maplesoft.com

Abstract

Blade roots are of the most stressed areas of a rotor in service. An in-service examination, whether performed manually or automated, is complex due to the geometries involved. The levels of probability of detection, repeatability, reliability are consequentially affected. The work is thus time consuming and impacts outage durations. This paper describes a way to handle and set this kind of examination on complex geometries. From the scope of examination and associated conditions, through to mathematical software (MapleSoft) and physical modelling tool (CIVA). The entire package (physical and mechanical) is completely pre-designed and evaluated prior to implementation. Advanced UT technologies are used to ensure efficiency, reliability, scanning simplification and shortest possible inspection duration.

Keywords: ultrasound, phase array, analytical geometry, Modelling , last stage blade roots serration , power generation .

1. Scope of examination and method

The last stage blade root examination (serration 1) of LP turbines is always a critical step in the assessment phase of the maintenance program. It is a difficult task , is time consuming and the reliability of data captured is critical in the process of plant condition assessment.

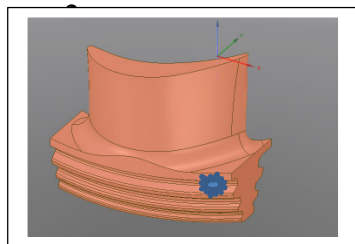


Fig. 1

Aerofoil intrados and extrados are the only accessible surfaces. First concave and convex serrations are suspected defect areas. Coordinates of defect region are; x:-40..140 mm, z: as per intrados or extrados curves, y: -27.16 first groove

Due to the lack of concentricity between inspection surfaces and suspect defect areas, maintaining optimal corner effect for detection requires continuously changing the shot conditions. Multi mechanical and physical conditions are necessary. The scanning conditions requires numerous and complex patterns that increase the risk of errors and complicates the analysis.

To overcome the complex conditions and to increase inspection confidence, the examination conditions are reconstructed through an analytical process that considers; scanning surfaces, curves of defect location and optimal shot conditions (MapleSoft). From these results, the optimal UT sensor locations, optimal UT settings, is achieved by modelling (CIVA), to pre-design a package able to carry out the examination with highest reliability, reducing operating time and providing results for immediate use.

2. Analysis of the examination conditions

2.1 Principles

Different factors influence the conditions of the examination among these are; the shape of defect areas, shape of scanning surfaces, shot conditions required for best detection.

To handle these fundamental factors and to accommodate all of them together, an analytical scenario is required to create the required details of the beam conditions. Beam conditions depend primarily on the scan surface relative to the target defect position that involves the tangent, normal, binormal, and incidence on targets. The use of 2D phased array with equipment offering different focal law features is essential. The mathematical formulas for the plotting of involved geometries and the shot positions, are the steps required in the fundamental analysis (MapleSoft). Subsequently the resultant physical conditions are used to build the specification of the scanning package (CIVA).

2.1.1 Digital pattern of scanning surface relative to defect curves

The matrix map is provided by CAD software. Through approximation module equation (3D, 2D) of surfaces, curves are obtained. For the aerofoil surfaces per the shape approximation is done according to quadric equations, last square method. For the defect curves the same approximation is performed.

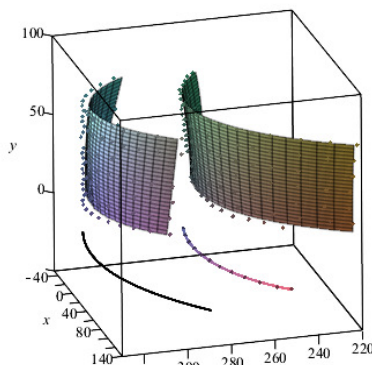


fig. 2

Intrados and extrados surface and respective extrados and intrados defect curves

Extrados surface equation:

$$-0.00553718025671160 x^2 - 0.000129365079345257 y^2 + 0.411469318496011 x - 0.00904761904957697 y + 322.809067229500$$

Intrados curve equation:

$$-0.00211998301071295 x^2 + 0.0103970066680208 x + 275.591147874800$$

$$z = -27.16$$

2.1.2 Shot conditions – optimised probe locations curve

The optimal beam condition to get a response from a defect is by corner effect. The assumption is that of an indication within the horizontal plane at a constant depth ($z=27.16$) to intersect the plane normal to the tangent plane. The beam vector targets the defect at 45° and includes the plane containing the binormal vector of the tangent and normal vector.

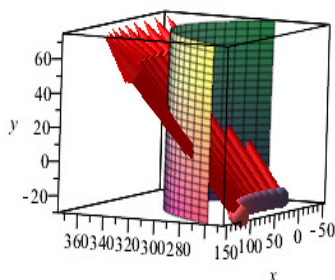


Fig. 3

For 45° incidence the beam vector is the sum of normal and binormal vector

The intersection curve on surface obtained (x parameter) by:

$$(x)e_x + (-0.00610651359164915 x^2 + 0.660855419603687 x + 52.9006313991360)e_y + (-0.00540606924018179 x^2$$

3. Skew effect

At each point on the optimised probe location, the target point on the defect curve is swept through a range achieved by skewing the beam vector. This is to provide an optimised response beam vector from any probable defect location. The response beam vector is built through symmetry and calculation of the plane containing the response from the optimised probe locations curve..

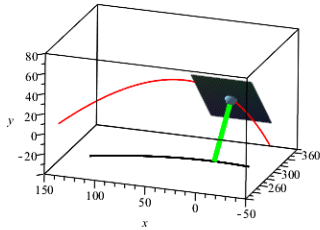


fig. 4. 0° Skew

Skew= 0°

T Sensor coordinates: $x=0\text{mm}$, $y=322\text{mm}$, $z=19\text{mm}$

Target point : $x=0\text{mm}$, $y=275\text{mm}$, $z=-27.16\text{mm}$

T Sensor tilt= 0° , pan = 0° , incidence in vertical plane on defect curve= 45° (plane containing the beam vector)

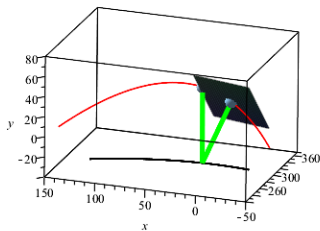


fig. 5 10° Skew

Skew= 10°

T Sensor coordinates: $x=0$, $y=322$, $z=19$

R Sensor coordinates: $x=31$ $y=328$ $z=28$

Target point : $x=12\text{mm}$ $y=275\text{mm}$ $z=-27.16\text{mm}$

T Sensor tilt= 0° , pan = 17°

R Sensor incidence in vertical plane on failure curve = 44°

4. Outputs from analytical stage

From the above the main input data required to set the parameters of the examination, are determined.

These include; pattern to locate sensor, beam behaviour: refraction, skew, tilt, pan, as well as the possibility to calculate the focal laws, if necessary

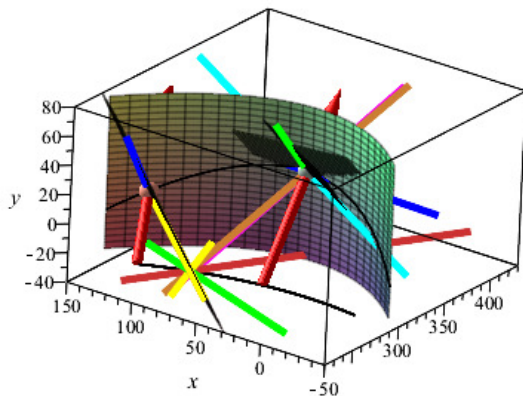


Fig. 6 Shot Build Graphic

General sketch to build a shot sequence:

Skewed T Sensor: Rose coloured Beam
Beam intersecting the surface on optimised curve in yellow

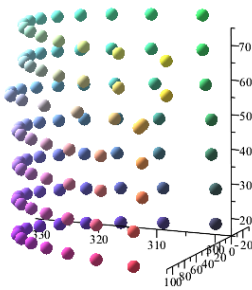
5. Sensor location package

The application below defines the layout of the final profile composition of the sensor belt to be installed along the optimised sensor location curve. It is the result of the optimised sensor location curve relative to the defect curve and when at each point the tangent direction change (\pm) compensates for any skew.

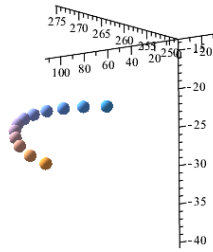
For application where surface examination is extrados and the defect curve is intrados:

- Plotting and Calculation is a function of scanning surface, defect curve, and resultant optimised sensor curve

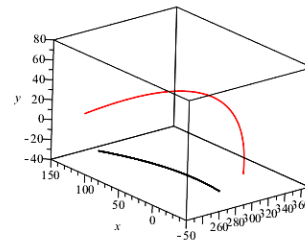
Below is illustrated the process for extrados sensor optimised curve relative to the intrados defect curve.



Scan Surface Plot
fig. 7



Defect Curve Plot
fig. 8



Optimised Sensor Curve
fig. 9

- Origin - location for the first sensor (4x4 elements, 5 MHz, skew $+10^\circ/-10^\circ$, foot print, 5x5mm)

The origin is selected on optimized sensor location curve, at the point corresponding to the horizontal tangent “t”

The groove extension covered by the scan with access from aerofoil is -15 to 115 mm.

The adjacent extensions of the groove are scanned from the shoulder of the blade.

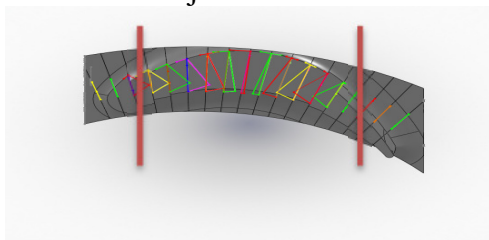
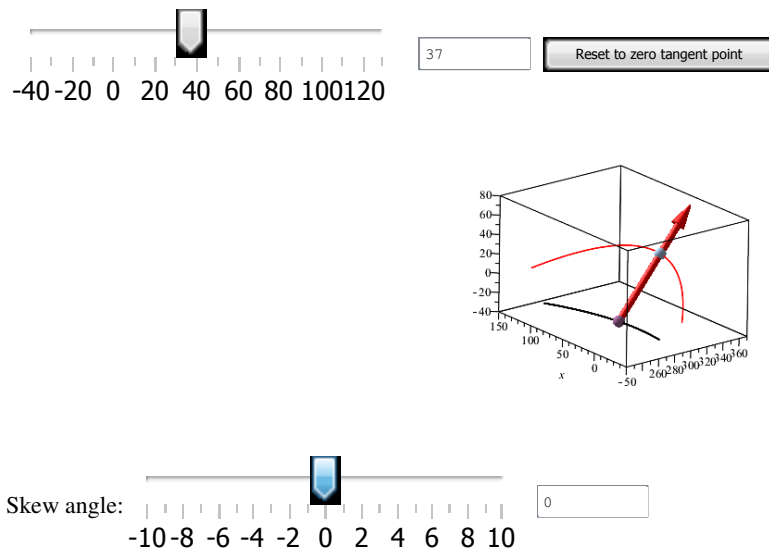


fig. 10

In this instance the origin point correspond to 37 mm.

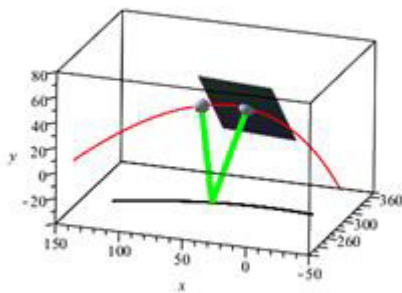
Example for Parameters for the optimized sensor curve:



.414930735229872, -27.16, 274.5265609: Coordinates on indication curves

Fig. 11

Example of range and T-R sensor positions



Eg. From location 37mm on optimised sensor location curve skew 10° Target on indication curve $x=42\text{mm}$, $r=272\text{mm}$, $z=-27.16\text{mm}$

Next sensor location for a skew 10 : $x: 67\text{mm}$, $r: 324\text{mm}$, $z: 29\text{mm}$

The skew of next sensor is defined -10°

From this location the same process is applied to get the required coverage

Fig. 12

Coordinates of the point on the indications curve: 44.32407938, -27.16, 271.887016093669

Coordinates of the new sensor: 71.08255220, 29.1987239641721, 323.71468

Angle between normal plane (beam vector) and tangent line: 9.73522667389432

Tilt angle: .2489501929

Skew angle at the second point: -10.018171780683

Tilt angle at the second point : 0.9226578598e-1

The sensor package is defined and summarized below. This package covers the area to be scanned without movement of the sensor. The array belt consists of 7 groups of 16 elements (112elts) that allows for a maximal coverage using skew -10° to $+10^\circ$. The groups are positioned in belt along the optimised sensor location curve.

data	T-2T-1		T-1T0			T0T1			T1T2			T2T3			T3T4			T4	
Skew range °	0	10	-10	0	10	-10	0	10	-10	0	10	-10	0	10	-10	0	10	-10	0
xp mm	-21	4	35	4	35	71	35	71	36	71	99	70	99	121	101	121	137	121	137
rp mm	311	323	311	324	330	324	330	323	330	323	308	323	308	291	307	291	274	307	274
zp mm	9	20	9	21	29	21	29	29	29	29	22	29	22	14	22	14	4	22	4
skew°	0	-10	-10	0	-10	-10	0	-10	-10	0	-10	-9	0	-9	-9	0	-9	-6	-3
tpr°	36			27			10				-9			-21			-27		-32
xi mm	-17	-8	-8	3	15	16	30	44	44	58	71	71	82	94	95	105	114	116	124
ri mm	274	275	275	275	275	275	273	271	271	269	265	265	261	257	257	253	248	248	244
zi mm	-27.16																		

Table a

This defined package utilises the potential capabilities of 2D arrays and enables the scanning to meet the inspection objectives.

The ultrasonic Modelling next defines the conditions of the beam sweep required to detect the flaws (type of focal laws)

3 Ultrasonic Modelling

The pre designed array belt for the extrados scan surface contains 7 arrays, though due to curvature only 6 arrays (maximum) can be adequately seated on the surface of the aerofoil. Scanning from the flat shoulder of the blade is done with existing conventional methods. The belt for the intrados scan surface has 5 arrays inserted (80elts) coverage $(-15\text{ mm}/90\text{mm})$

T-2(-21 mm)1

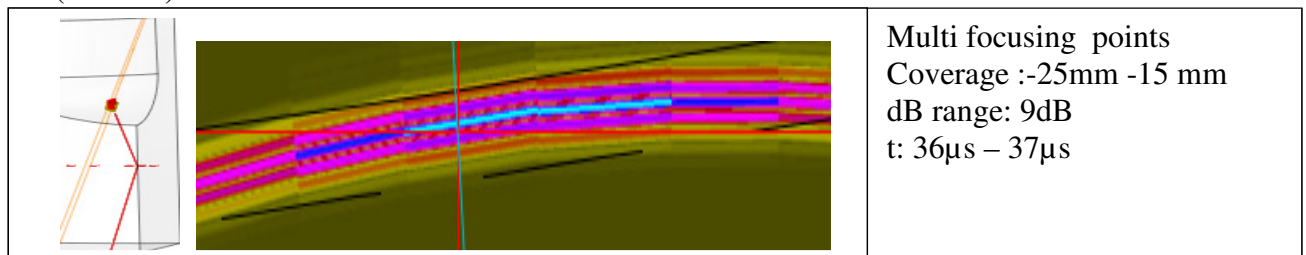


Fig. 13

T-2 T-1(-21mm-4mm)

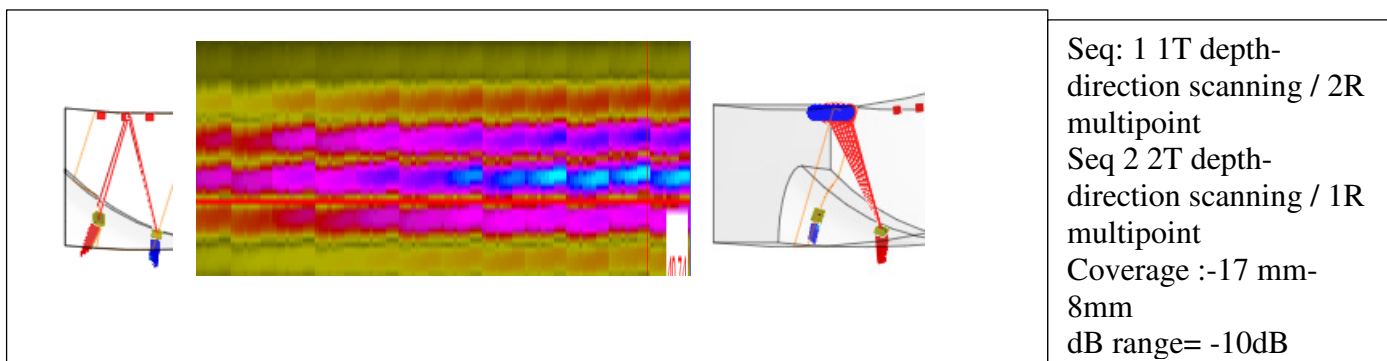


Fig. 14

T-1(4mm)2

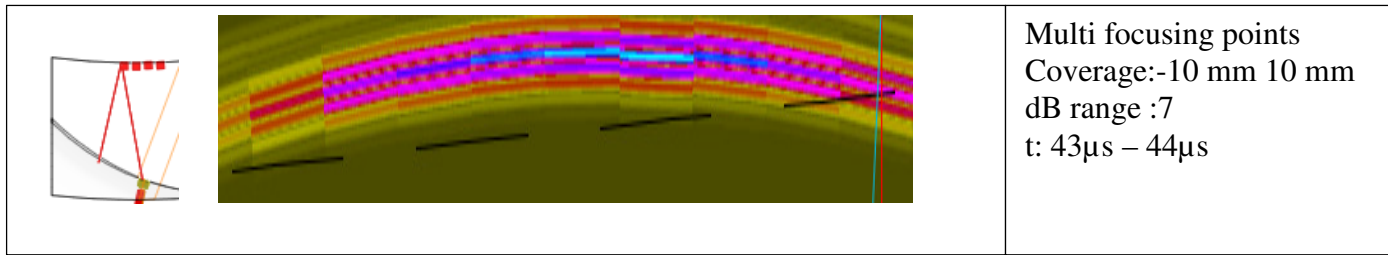


Fig.15

T-1 T-0(4mm-37mm)

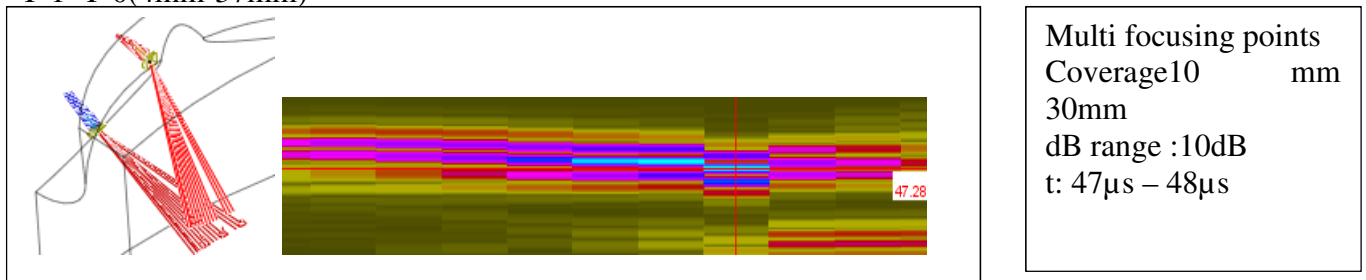


Fig. 16

T0 (37mm)3

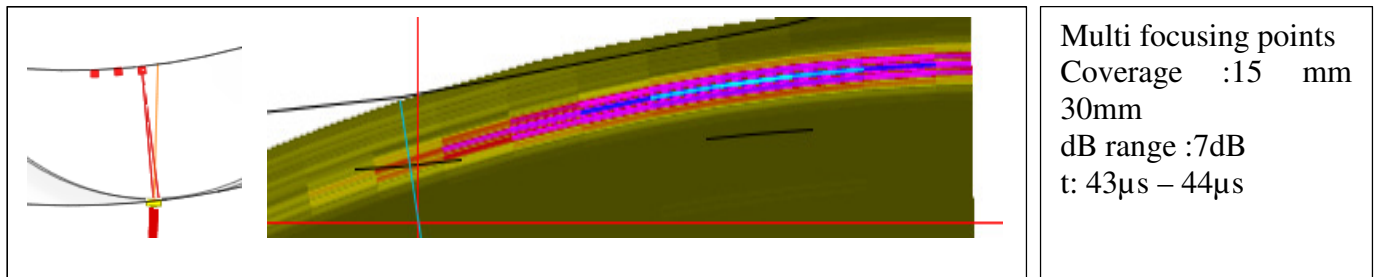


Fig. 17

T0 T1 (37mm 71mm)

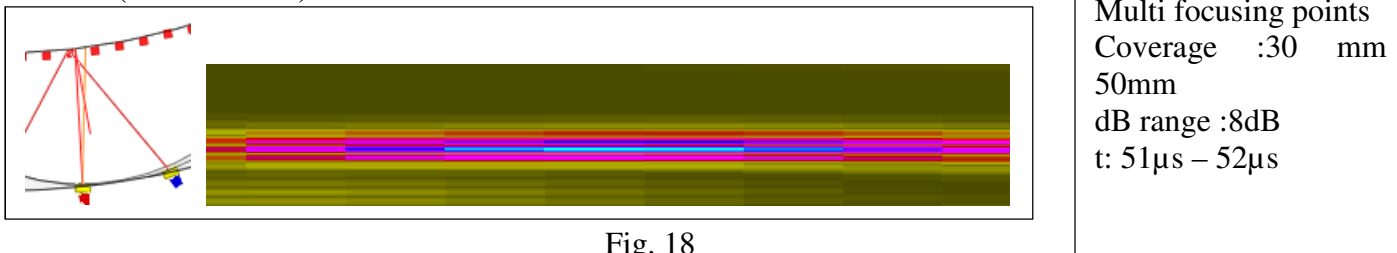


Fig. 18

T1 (71 mm)4

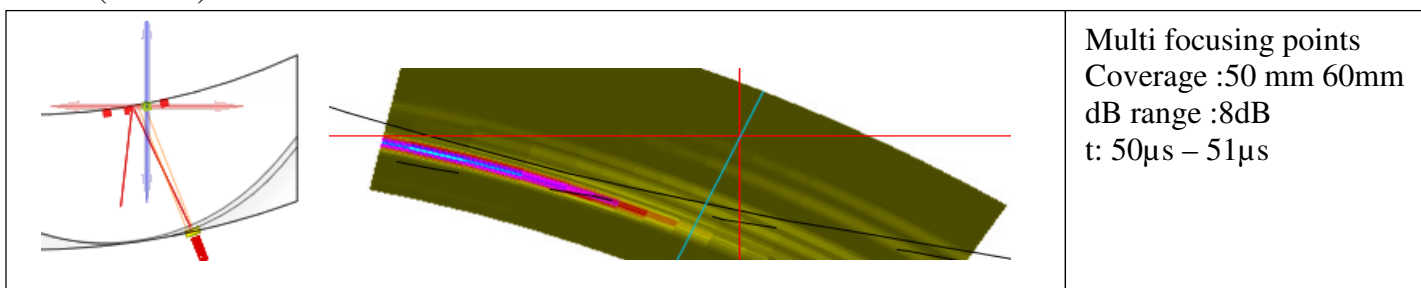


Fig. 19

T1-T2(71 mm-100mm)

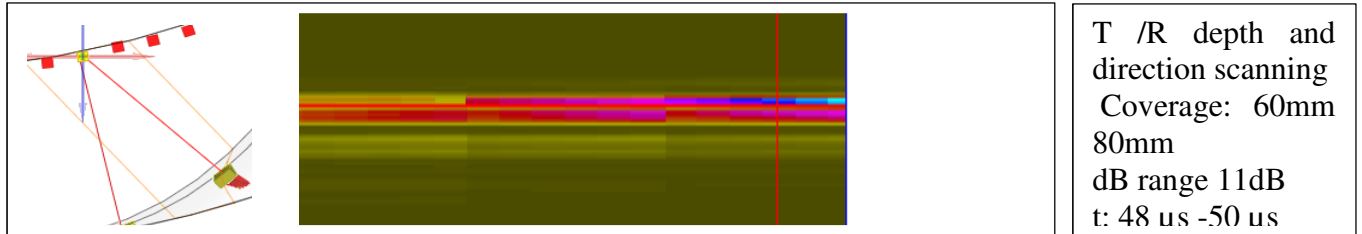


Fig. 20

T2 (100 mm) 5

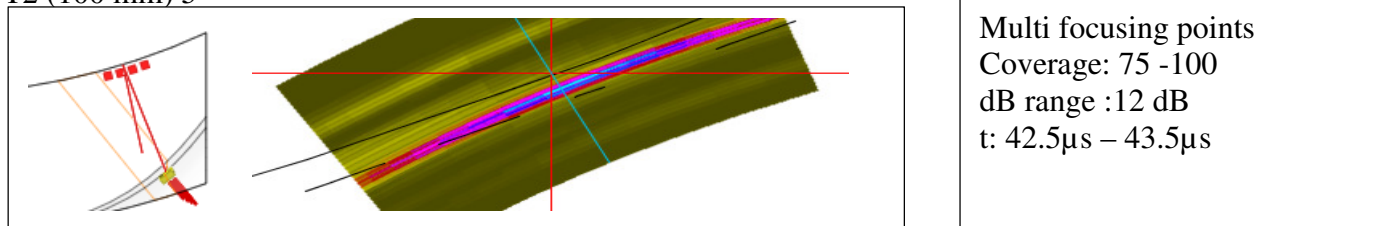


Fig. 21

Different modes of focusing have been evaluated and it was found that the most reliable, for pulse echo, was to use multipoint focusing. When using tandem the standard combination of focusing provides adequate scans results. The choice of soft skew and squint is governed by the sensor location on the optimised position.

The next update of application is the calculation of step per step between 2 sensors of these angles.

4 Conclusion

The existing advanced software tools allow and facilitate the understanding of complex examinations.

- ✚ Full analysis: geometrical Modelling – ray behaviour with main numerical parameters
- ✚ Predesign of sensor package
- ✚ Ultrasonic behaviour to verify and validate assumptions: defect response
- ✚ Accurate specifications to design the scanning equipment and process : essential parameters
- ✚ Efficient and powerful use of advanced tools: 2D PA – Array belt - advanced focusing: multi point depth and direction scanning
- ✚ Procedures for data capture and analysis

This method, not only helps in the understanding of the scope and then accurately designing the inspection process, but gives tools to quantify any deviation from the inspection specification by replaying from the captured data with the developed applications.

This study specifies a new toll that can be used in this type of inspection. An array belt that avoids the mechanical movement of the scan probes. The scan is achieved in the single placement of the belt array on the blade and could possibly allow both sides of the blade to be scanned simultaneously. The cartography allows display and print on line for immediate analysis, reporting and possible replay.

Studies to construct the array belt and plugging device are ongoing.

The projected operating time forecast to perform a scan on one disc 44 blades is 2 mandays inclusive of reporting. This manual examination presently requires 6mandays.

The developed application for blades can also be extended to cover other types of geometry.